Picosecond Third Harmonic Generation in β-BaB_2O_4 and Calcite

A. Penzkofer, P. Qiu, and F. Ossig*

Naturwissenschaftliche Fakultät II-Physik, Universität Regensburg,
D-8400 Regensburg, Fed. Rep. of Germany
*On leave from Shanghai Institute of Optics and Fine Mechanics,
Academia Sinica, Shanghai, Peop. Rep. of China

1. Introduction

Phase-matched third harmonic generation has been achieved in metal vapors [1,2] inert gases [3], organic dyes [4-6], liquid crystals [7] and birefringent crystals [8-14]. Third harmonic light may be generated by the direct third-order nonlinear interaction, $\nu_L+\nu_L+\nu_L\rightarrow\nu_3$, due to the third-order nonlinear susceptibility $\chi^{(3)}_{THG}$, or it may be generated by cascading the second harmonic generation, $\nu_L+\nu_L\rightarrow\nu_2$, and the frequency mixing, $\nu_2+\nu_L\rightarrow\nu_3$. The second harmonic generation and the frequency mixing are due to the second-order nonlinear susceptibilities $\chi^{(2)}_{SHG}$ and $\chi^{(2)}_{FM}$. Phase-matching, $\Delta k=0$, is necessary for efficient third harmonic light generation. In birefringent crystals it is achieved by crystal orientation and angle tuning. In crystals with inversion center only direct third harmonic generation is allowed while in crystals without inversion center cascading and mixed (direct and cascading) third harmonic generation are possible. A double phase-matching of the second harmonic generation and the frequency mixing requires two separately oriented crystals in series. The subsequent phase-matched second harmonic generation and phase-matched frequency mixing is most efficient and is widely used [15]. The various phase-matching schemes for third harmonic generation in negative uniaxial birefringent crystals are summarized in Table 1.

Table 1 Single and double phase-matched angle-tuned generation of third-harmonic light in negative uniaxial birefringent crystals ($n_e<n_o$). D = direct. C = cascading. D+C = mixed. IC = inversion center.

Crystal	Process	Phase-matching	Interaction		Contribution
single crystal, single phase-matched					
with IC	D	$\Delta k_{THG}=0$	type I	$o_L o_L o_L\rightarrow e_3$	$\chi^{(3)}_{eff,THG}$
			type II	$o_L o_L e_L\rightarrow e_3$	
			type III	$o_L e_L e_L\rightarrow e_3$	
without IC	C	$\Delta k_{SHG}=0, \Delta k_{FM}\neq 0$ [a]	type I	$o_L o_L\rightarrow e_2$	$\chi^{(2)}_{eff,SHG}$
			type II	$o_L e_2\rightarrow e_2$	
	C	$\Delta k_{SHG}\neq 0, \Delta k_{FM}=0$	type I	$o_2 o_L\rightarrow e_3$	$\chi^{(2)}_{eff,FM}$
			type II	$o_2 e_L\rightarrow e_3$	
			type III	$e_2 o_L\rightarrow e_3$	
	D+C	$\Delta k_{THG}=\Delta k_{SHG}+\Delta k_{FM}=0$	type I	$o_L o_L o_L\rightarrow e_3$	$\chi^{(3)}_{eff,THG}+\chi^{(2)}_{eff,cas}$
			type II	$o_L o_L e_L\rightarrow e_3$	
			type III	$o_L e_L e_L\rightarrow e_3$	
two crystals, double phase-matched					
without IC	C	$\Delta k_{SHG,1}=0$ and $\Delta k_{FM,2}=0$	type I	$oo\rightarrow e$	1: $\chi^{(2)}_{eff,SHG}$ and 2: $\chi^{(2)}_{eff,FM}$
			type II	$oe\rightarrow e$	

a) Cascading third harmonic generation with $\Delta k_{SHG}=0$ is less efficient compared to $\Delta k_{FM}=0$ [13].

Springer Proceedings in Physics, Vol. 36
Nonlinear Optics of Organics and Semiconductors
Editor: T. Kobayashi

In this paper the single phase-matched third harmonic generation in single crystals of calcite and β-BaB_2O_4 is studied. Calcite is a negative uniaxial crystal with inversion center (trigonal system, space group $R\bar{3}c$, point group $\bar{3}m$). β-BaB_2O_4 is a newly developed negative uniaxial crystal without inversion center [16,17] (trigonal system, space group R3, point group 3; a higher symmetry of R3c and 3m is stated in [18]). The large effective second harmonic coefficients, the wide transparent waveband (190 - 3500 nm), and the high damage threshold make BBO very important for second harmonic generation and frequency mixing in the ultraviolet spectral region [19-24]. β-BaB_2O_4 was applied successfully in the second harmonic generation of femtosecond pulses [25,26].

Table 2 gives a list of crystals that have been applied to the phase-matched third harmonic generation in a single crystal.

Table 2 Realized phase-matched third harmonic generation in single crystals. All crystals are negative uniaxial. D = direct. D+C = mixed.

Crystal	Class	Interaction	Laser	λ_L [nm]	References
Calcite	trigonal, $R\bar{3}c$	D	Q-switched	694.3	8,9
			Q-switched	1060	11,14
			Mode-locked	1054	this work
KDP	tetragonal, $\bar{4}2m$	D+C	Q-switched	1064	11
ADP	tetragonal, $\bar{4}2m$	D+C	Q-switched	1060	10
			Mode-locked	1060	10
β-BaB_2O_4	trigonal, R3(R3c)	D+C	Mode-locked	1054	this work

2. Fundamentals

The geometrical arrangement of phase-matched third harmonic generation in a single crystal is sketched in Fig.1. The angle Θ between the crystal fixed z-axis (optic axis) and wave-vector $\vec{k}_L(\|\vec{k}_3)$ is adjusted to phase-matching. α_L and α_3 are the walk-off angles between the ray directions of extraordinary and ordinary polarized light.

Collinear phase-matching of mixed or direct THG requires

$$\Delta k = k_{e3} - k_{aL} - k_{bL} - k_{cL} = 0 \; ; \qquad (1)$$

a,b,c indicate the polarizations o or e of the fundamental waves. In the case of type-II phase-matching it is $k_{3e}-2k_{oL}-k_{eL}=0$. The wave-vectors are related to the refractive indices n by $k=2\pi n\nu/c_0$ where ν is the frequency and c_0 is the vacuum light velocity. The ordinary refractive index n_o is independent of crystal orientation. The extraordinary refractive index depends on the polar angle Θ by

$$n_e(\Theta) = \frac{n_o n_e}{(n_e^2\cos^2\Theta + n_o^2\sin^2\Theta)^{1/2}} \; ; \qquad (2)$$

n_o and n_e are the principal refractive indices.

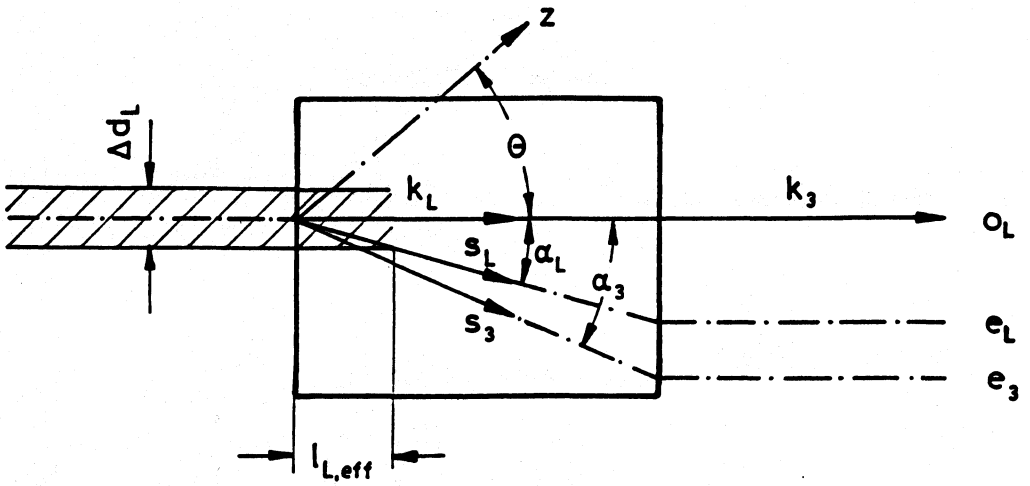

Fig.1 Schematic geometrical arrangement

The walk-off angle α_L limits the overlap length of the o und e pump laser components in the case of type-II and type-III phase-matching to

$$\ell_{L,eff} \simeq \frac{\Delta d_L}{2\alpha_L} \tag{3}$$

where Δd_L is the pump pulse beam diameter. The walk-off angle α_3 allows third harmonic generation over the whole crystal length but amplifying interaction between pump and third harmonic light occurs only within an effective length

$$\ell_{3,eff} \simeq \frac{\Delta d_L}{2\alpha_3} \quad . \tag{4}$$

For femtosecond pulses the temporal overlap of the o and e pump pulse components of type-II and type-III phase-matched crystals may be limited by the group velocity dispersion. The group refractive index is

$$n_g = \frac{n}{1 - \frac{\nu}{n}\frac{\partial n}{\partial \nu}} \quad . \tag{5}$$

The time delay between ordinary and extraordinary rays is given by $(\delta t/\delta \ell)_{oLeL} = [n_{goL} - n_{geL}(\Theta)]/c_0$ and the overlap length is limited to

$$\ell_o \simeq \frac{\Delta t_L}{(\delta t/\delta \ell)_{oLeL}} \quad . \tag{6}$$

The duration of the generated third harmonic pulse is given approximately by

$$\Delta t_3 \simeq [\tfrac{1}{3}\Delta t_L^2 + (\delta t/\delta \ell)^2_{e3oL}\,\ell_I^2\,]^{1/2} \tag{7}$$

where ℓ_I is the shorter length of ℓ, ℓ_o, and $\ell_{L,eff}$.

The energy conversion efficiency of third harmonic generation is given by [12,13]

$$\eta_E = \kappa \ell^2 I_{0L}^2 |\chi_{eff}|^2 \frac{\sin^2(\Delta k \ell/2)}{(\Delta k \ell/2)^2} \; f(\Delta d_L, \Delta\Theta_L, \Delta\nu_L, \Delta t_L) \tag{8}$$

κ comprises constant factors. The function f takes care of the reduction of conversion efficiency due to the finite beam diameter Δd_L, the divergence $\Delta\Theta_L$, the spectral width $\Delta\nu_L$, and the pulse duration Δt_L of the pump pulse.

3. Crystal data

The dispersion of the principle refractive indices n_o and n_e of calcite [27] and BBO [19] are depicted in Fig.2. The transmissions T are shown in Fig.3. The type-I, II, and III phase-matching angles of direct THG in calcite and of mixed THG in BBO are plotted in Fig.4. The corresponding walk-off angles α_L and α_3 are diagrammed in Fig.5.

The angular dependence $\eta_E(\Theta)/\eta_E(\Theta_{PM})$ of BBO is shown in Fig.6a for λ_L = 1.054 µm ($\Delta\Theta_L$=0, $\Delta\nu_L$=0, Δd_L=∞). $\Delta\Theta_{1/2}$ is the FWHM of the angular detuning curve.

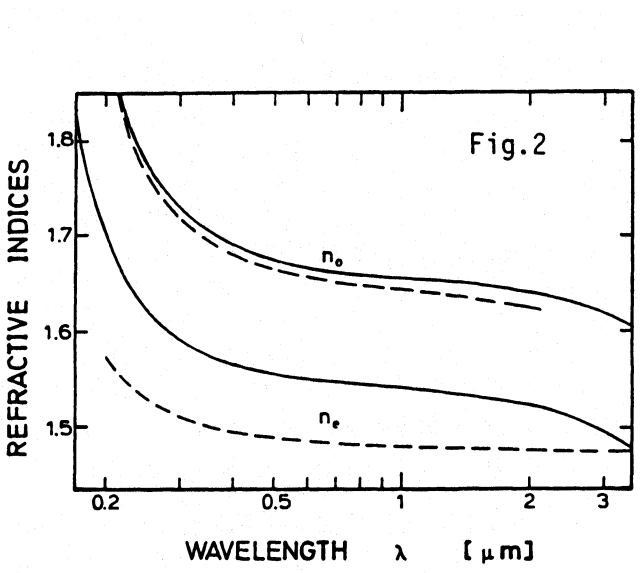

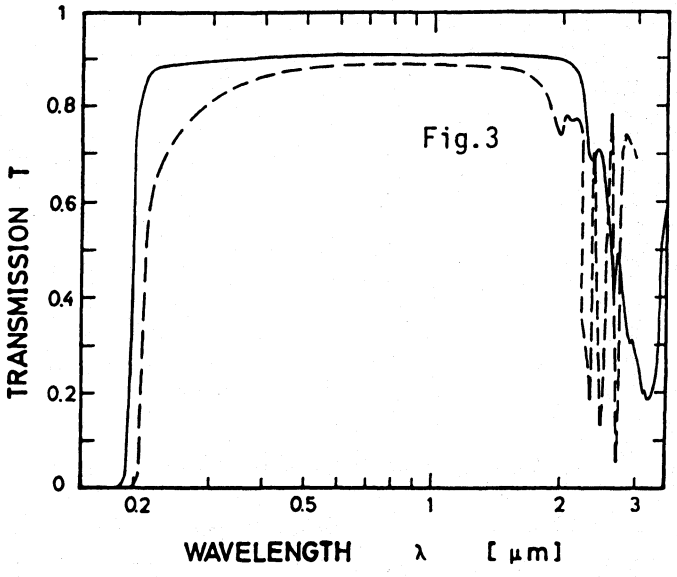

Fig. 2 Refractive indices of β-BaB_2O_4 (solid)[19] and calcite (dashed)[27].

Fig.3 Spectral transmission of β-BaB_2O_4 (ℓ = 6 mm, solid) and calcite (ℓ = 33 mm, dashed).

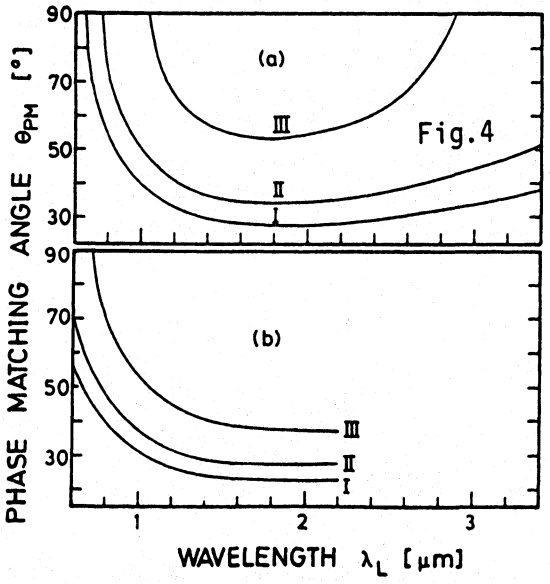

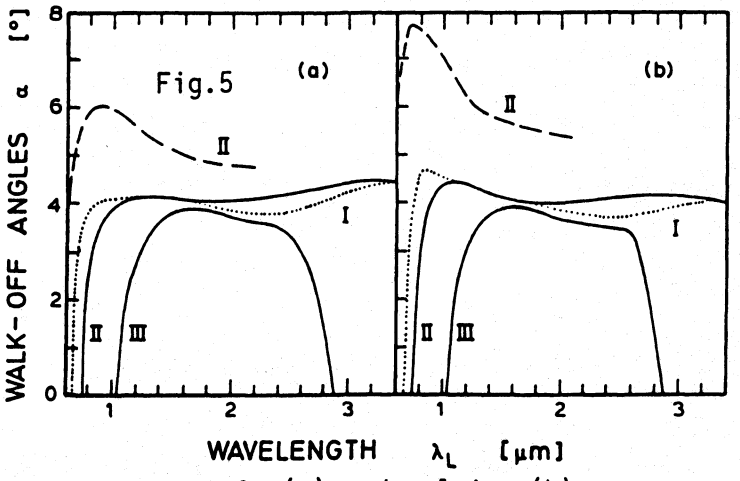

Fig.4 Type-I, II, and III phase-matching in β-BaB_2O_4 (a) and calcite (b).

Fig.5 Walk-off angles α_L(a) and α_3(b) of BBO (solid and dotted) and calcite (dashed, only type-II is shown).

$\Delta\Theta_{1/2}$ is inverse proportional to the crystal length ℓ. $\Delta\Theta_{1/2}\ell$ versus wavelength is plotted in Fig.7 for calcite and BBO. The internal divergence of the pump laser radiation, $\Delta\Theta_{L,int}$, should be less than $\Delta\Theta_{1/2}$ in order to avoid remarkable loss of efficiency (external divergence angle $\Delta\Theta_L \approx n_{oL}\Delta\Theta_{L,int}$).

The frequency dependence $\eta_E(\nu)/\eta_E(\nu_L)$ at a fixed angle is similar to the angular dependence at a fixed wavelength. $\eta_E(\nu)/\eta_E(\nu_L)$ of BBO is depicted in Fig.6b ($\Delta\Theta_L$=0, $\Delta\nu_L$=0, Δd_L=∞). Phase-matching is adjusted to $\bar{\nu}^{-1} = \lambda_L$ = 1.054 µm. $\Delta\nu_{1/2}$ is the FWHM of the spectral detuning curve. $\Delta\nu_{1/2}$ is inverse proportional to the crystal length ℓ. $\Delta\bar{\nu}_{1/2}\ell$ versus wavelength is displayed in Fig.8. The spectral width of the pump laser $\Delta\nu_L$ should be less than $\Delta\nu_{1/2}$ in order to avoid remarkable loss of efficiency.

The group velocity dispersion limits the temporal overlap (Eqs.6 and 7). The curves of $(\delta t/\delta\ell)_{oLeL}$ and $(\delta t/\delta\ell)_{e3oL}$ are depicted in Fig.9a and 9b, respectively.

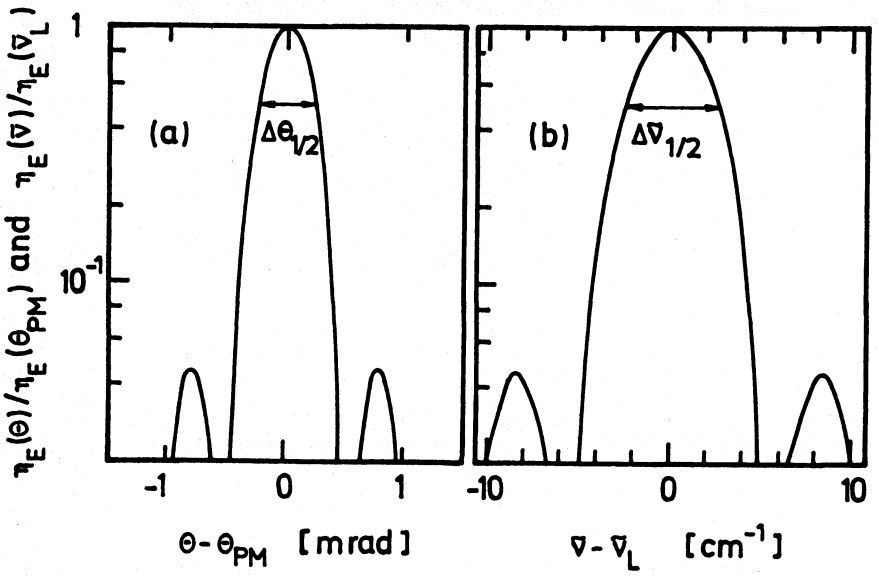

Fig.6 Angular (a) and spectral (b) detuning curves of β-BaB_2O_4 at λ_L = 1.054 µm for type-II phase-matched mixed THG (ℓ = 0.72 mm).

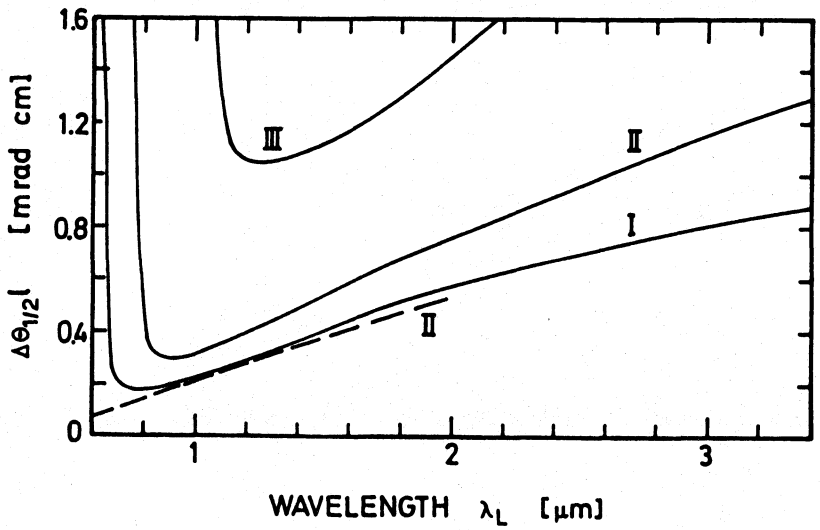

Fig.7 Halfwidth of angular tuning curves for BBO (solid) and calcite (dashed, only type-II). Mixed THG.

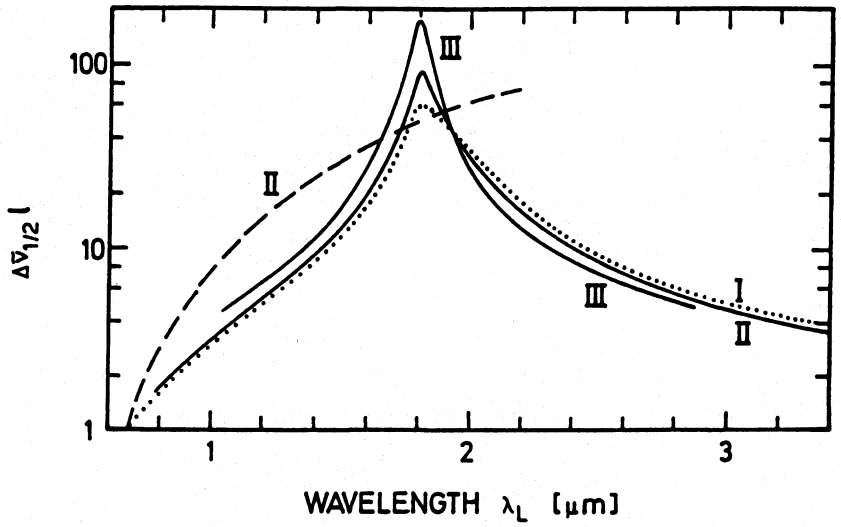

Fig.8 Halfwidth of spectral tuning curves for BBO (solid and dotted) and calcite (dashed, only type-II is shown). Mixed THG.

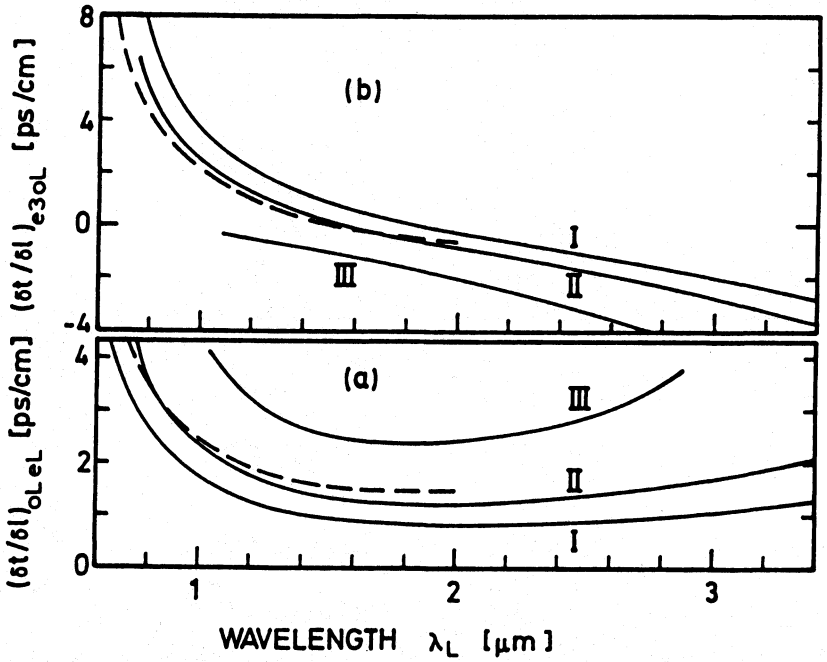

Fig.9 Time delays $(\delta t/\delta \ell)_{oLeL}$ (a) and $(\delta t/\delta \ell)_{e3oL}$ (b) for mixed THG in BBO (solid) and direct THG in calcite (only type-II is shown).

4. Experimental

The experimental setup is shown in Fig.10. Single picosecond light pulses of a passively mode-locked Nd-phosphate glass laser ($\Delta t_L \approx 5$ ps, $\lambda_L = 1.054$ μm) are used as pump pulses. The energy conversion efficiency of third harmonic light versus input pump pulse peak intensity is measured and the angular detuning curves are determined. The calcite crystal is 2 cm long and the length of the β-BaB_2O_4 crystal is $\ell = 7.2$ mm. In some calcite measurements a cylindrical lens is inserted to generate a line-focus which increases the light intensity at the crystal without increasing the relevant laser divergence $\Delta\Theta_L$ in the plane spanned by the optic axis and the light propagation direction.

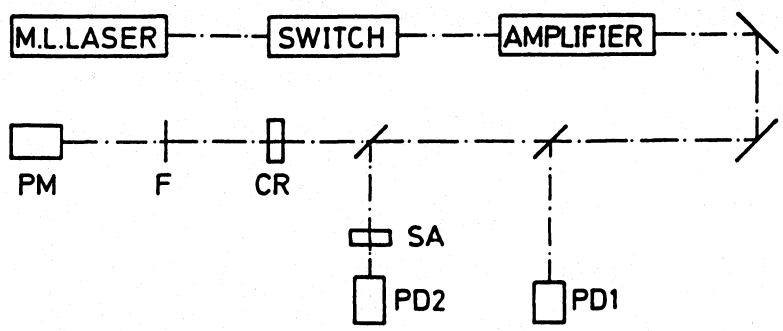

Fig.10 Experimental setup. PD1, PD2, photodetectors. SA, saturable absorber (Kodak No.9860) for peak intensity detection [28]. CR, crystal. F, filter. PM, photomultiplier.

5. Results

Type-II phase-matched mixed (BBO) and direct (calcite) THG are investigated. The angular detuning curves $\eta_E(\Theta)/\eta_E(\Theta_{PM})$ of BBO and calcite are shown in Fig.11. For BBO the spectral width of the pump laser is $\Delta\tilde{\nu}_L = 10\ cm^{-1}$. In the case of calcite two curves are depicted for $\Delta\tilde{\nu}_L = 10\ cm^{-1}$ and $\Delta\tilde{\nu}_L = 40\ cm^{-1}$ (self-phase modulated pulses).

The phase-matched THG energy conversion efficiency versus pump pulse peak intensity is depicted in Fig.12. At the highest intensities applied conversion efficiencies of $\eta_E \simeq 0.01$ ($I_{0L} = 5\times10^{10}$ W/cm²) and $\eta_E \simeq 8\times10^{-5}$ ($I_{0L} = 10^{11}$ W/cm²) have been obtained for BBO and calcite, respectively. The damage threshold of calcite is $I_{th,C} > 10^{13}$ W/cm² and the damage threshold of BBO is $I_{th,B} \approx 10^{12}$ W/cm² [18,22] for single pulses of 5 ps duration. At pump pulse intensities slightly below the damage threshold very high conversion efficiencies are expected in both crystals.

The effective nonlinear susceptibilities $\chi^{(3)}_{eff}$ are determined by comparison of the measured energy conversion efficiencies η_E with calculations (Eq.5). The obtained values are listed in Table 3 together with other crystal parameters. A

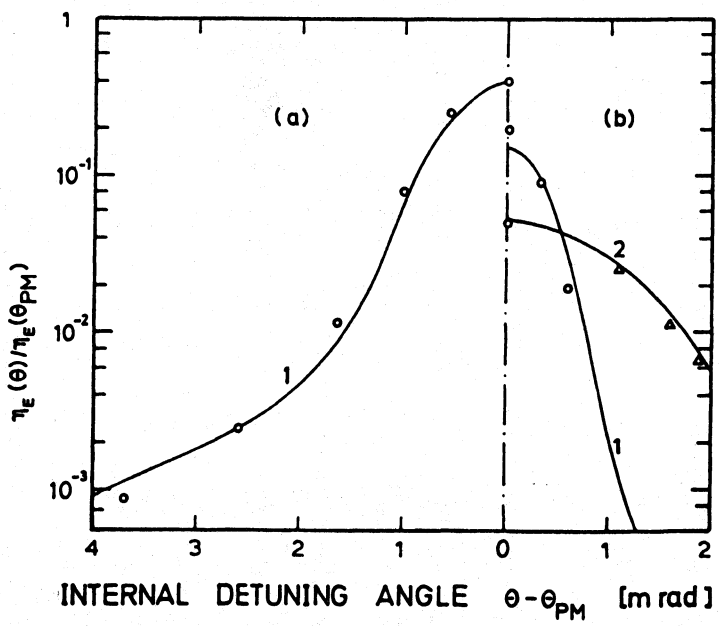

Fig.11 THG conversion efficiency versus detuning angle for BBO of 0.72 cm length (a) and calcite of 2 cm length (b). $\Delta\Theta_L = 5\times10^{-4}$ rad. (1,o), $\Delta\tilde{\nu}_L = 10\ cm^{-1}$. (2,Δ), $\Delta\tilde{\nu}_L = 40\ cm^{-1}$. Type-II phase-matching.

detailed analysis of the effective susceptibilities indicates that $\chi^{(3)}_{eff,THG}$ and $\chi^{(2)}_{eff,cas}$ are of the same order of magnitude for BBO [13].

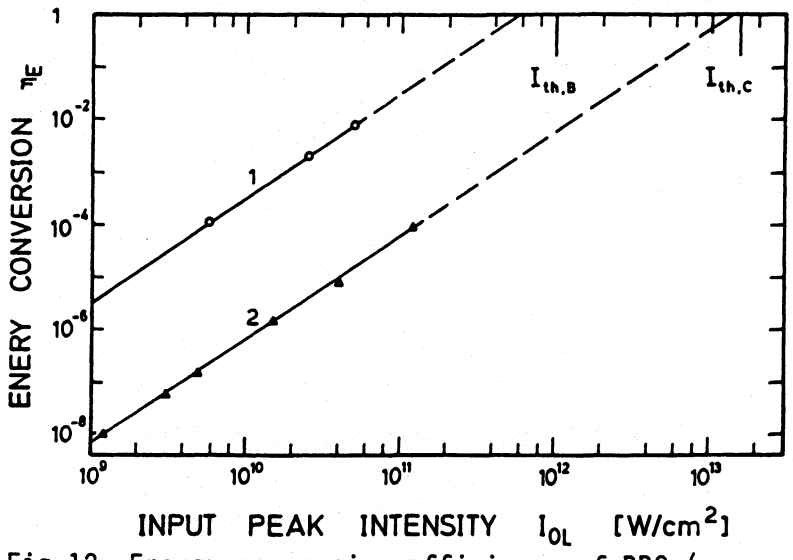

Fig.12 Energy conversion efficiency of BBO (curve 1,o; ℓ = 7.2 mm) and calcite (curve 2,Δ; ℓ = 2 cm). Type-II phase-matching. $\Delta\Theta_L = 10^{-4}$ rad. $\Delta\tilde{\nu}_L$ = 20 cm^{-1}. The damage thresholds $I_{th,B}$ (BBO) and $I_{th,C}$ (calcite) are indicated.

Table 3 Phase-matched third harmonic generation of picosecond pulses of a Nd-phosphate glass laser in calcite (ℓ = 2 cm) and β-BaB_2O_4 (ℓ = 7.2 mm). Δt_L = 5 ps, λ_L = 1.054 μm.

Parameter		Calcite	β-BaB_2O_4
System		trigonal	trigonal
Point group		$\bar{3}$m	3 (3m)
Space group		R$\bar{3}$c	R3 (R3c)
Process		D	D + C
Phase-matching		type-II (ooe→e)	type-II (ooe→e)
Θ_{PM}	[°]	35.96	47.4
$\Delta\Theta_{1/2}\,\ell$	[rad cm]	2.3×10^{-4}	3.4×10^{-4}
$\Delta\tilde{\nu}_{1/2}\,\ell$		8.8	3.7
α_3	[°]	6.75	4.45
α_L	[°]	5.85	4.05
$(\delta t/\delta\ell)_{e3oL}$	[ps cm^{-1}]	1.7	2.0
$(\delta t/\delta\ell)_{oLeL}$	[ps cm^{-1}]	2.2	2.1
$\chi^{(3)}_{eff,THG}$	[m^{2}V^{-2}]	3×10^{-24}	6.4×10^{-23}
$\chi^{(2)}_{eff,cas}$	[m^{2}V^{-2}]	-	6.6×10^{-23}
$\chi^{(3)}_{eff}$	[m^{2}V^{-2}]	3×10^{-24} (2.1×10^{-16} esu)	1.3×10^{-22} (9.2×10^{-15} esu)
η_E		8×10^{-5} a)	0.01 b)
I_{th}	[W cm^{-2}]	$\gtrsim 10^{13}$	~ 10^{12}
$\eta(I_{th})$		→ 1	→ 1

a: $I_{0L} = 10^{11}$ W/cm^2. b: $I_{0L} = 5\times10^{10}$ W/cm^2.

References

1. J.F. Reintjes: In Laser Handbook, ed. by M. Bass and M.L. Stitch, Vol.5 (North-Holland, Amsterdam, 1985) Ch.1.
2. C.R. Vidal: In Tunable Lasers, ed. by F.L. Mollenauer and J.C. White (Springer, Berlin, Heidelberg, 1987) p. 57.
3. A.H. Kung, J.F. Young, S.E. Harris: Appl. Phys. Lett. 22, 301 (1973).
4. P.P. Bey, J.F. Guiliani, H. Rabin: IEEE J. Quant. Electron. QE-7, 86 (1971).
5. J.C. Diels, F.P. Schäfer: Appl. Phys. 5, 197 (1974).
6. A. Penzkofer, W. Leupacher: Opt. Quant. Electron. 20, 222 (1988).
7. J.W. Shelton, Y.R. Shen, Phys. Rev. Lett. 26, 538 (1971).
8. R.W. Terhune, P.D. Maker, C.M. Savage: Appl. Phys. Lett. 2, 54 (1963).
9. P.D. Maker, R.W. Terhune: Phys. Rev. 137, A801 (1965).
10. C.C. Wang, E.L. Baardsen: Appl. Phys. Lett. 15, 396 (1969).
11. S.A. Akhmanov, L.B. Meisner, S.T. Parinov, S.M. Saltiel, V.G. Tunkin: Sov. Phys. JETP 46, 898 (1977).
12. A. Penzkofer, F. Ossig, P. Qiu: Appl. Phys. B, to be published.
13. P. Qiu, A. Penzkofer: Appl. Phys. B45, 225 (1988).
14. A.P. Sukhorukov, I.V. Tomov, Sov. Phys. JETP 31, 872 (1970).
15. D. Eimerl, IEEE J. Quant. Electron. QE-23, 575 (1987).
16. C. Chen, B. Wu, A. Jiang, G. You: Sci. Sinica (Ser.B) 28, 235 (1985).
17. A. Jiang, F. Cheng, Q. Lin, C. Chen, Y. Zheng: J. Cryst. Growth 79, 963 (1986).
18. D. Eimerl, L. Davis, S. Velsko, E.K. Graham, A. Zalkin: J. Appl. Phys. 62, 1968 (1987).
19. K. Kato, IEEE J. Quant. Electron. QE-22, 1013 (1986).
20. K. Miyarzaki, H. Sakai, T. Sato: Opt. Lett. 11, 797 (1986).
21. P. Lokai, B. Burghardt, D. Basting, W. Mückenheim, Laser und Optoelektronik 19, 296 (1987).
22. H. Schmidt, R. Wallenstein: Laser und Optoelektronik 19, 302 (1987).
23. R.S. Adhav, S.R. Adhav, J.M. Pelaprat: Laser Focus 23/9, 88 (1987).
24. J.T. Lin, C. Chen, Laser Focus 23/11, 59 (1987).
25. Y. Ishida, T. Yajima: Opt. Commun. 62, 197 (1987).
26. K.L. Cheng, W. Bosenberg, F.W. Wise, I.A. Walmsley, C.L. Tang: Appl. Phys. Lett. 52, 519 (1988).
27. American Institute of Physics Handbook, 3rd ed., ed. by D.E. Gray (McGraw-Hill, New York, 1972) p. 6-20.
28. A. Penzkofer, D. von der Linde, and A. Laubereau, Opt. Commun. 4, 377 (1972).